ligands and should have little impact on the NH_3 metal bonding.

Thus, as pointed out before, E and A_2 should be very close in energy (or mixed) and very hard to distinguish insofar as our experiments are concerned.

During the photolysis of *trans*-$[Ru(NH_3)_4P(OEt)_3CO]^{2+}$, CO is exclusively labilized on the *z* axis. During the photolysis of the *cis*-$[Ru(NH_3)_4(isn)L]^{2+}$ complex ions, the ligand preferentially labilized is the weaker π-acceptor ligand.[14]

The $E^{\circ\prime}$ for the Ru(III)/Ru(II) couple in the complex *trans*-$[Ru(NH_3)_4P(OEt)_3H_2O]^{3+/2+}$ is 0.46 V.[4] Since the oxidation of *trans*-$[Ru(NH_3)_5CO]^{2+}$ is only observed[21] at potentials higher than +1.0 V, one infers that CO stabilizes Ru(II) through the back-bonding interaction more than $P(OEt)_3$ does.[22]

Triethyl phosphite is a moderate σ base.[6] Therefore for the $P(OEt)_3$ system a synergism is possible between the σ and π components strengthening the Ru(II) → P(III) bond. In fact, the activation enthalpies for the thermal reaction

$$trans\text{-}[Ru(NH_3)_4P(OEt)_3L]^{2+} + H_2O \xrightarrow{k_{-1}} trans\text{-}[Ru(NH_3)_4P(OEt)_3H_2O]^{2+} + L$$

are 18 and 29 kcal/mol for L = CO and $P(OEt)_3$, respectively.[4,14]

On excitation from the ground state to the LEES, one electron is promoted from a $d\pi$ orbital to a σ^* orbital. This electron transfer would destabilize the Ru(II)-$P(OEt)_3$ and Ru(II)-CO bonds in two different ways: first, weakening the σ bonds Ru(II)-$P(OEt)_3$ and Ru(II)-CO as a consequence of the electron density increase on the *z* axis and, second, weakening the π bonds Ru(II)-CO and Ru(II)-$P(OEt)_3$. Since the Ru(II)-CO bond is almost only π in character,[14] this bond will be more sensitive than Ru(II)-$P(OEt)_3$ to the depopulation of t_{2g} orbitals and therefore more easily broken.

The relevance of σ and π components in the Ru(III)/Ru(II)-L bond is well illustrated in the chemistry of the systems[4,22-24] *trans*-$[Ru(NH_3)_4(P(OEt)_3)_2]^{2+}$ and *trans*-$[Ru(NH_3)_4P(OEt)_3H_2O)]^{3+}$, $[Ru(NH_3)_5CO]^{2+}$ and $[Ru(NH_3)_5N_2]^{2+}$. The last two systems, where the Ru(II)-L bond is mainly due the back-bonding Ru(II) → L, easy loss of N_2 and CO upon oxidation occurs since these ligands are not able to donate σ electrons to the Ru(III) center. However due to the $P(OEt)_3$ biphilicity,[6,7] the complex ions *trans*-$[Ru(NH_3)_4(P(OEt)_3)_2]^{3+}$ and *trans*-$[Ru(NH_3)_4P(OEt)_3H_2O]^{3+}$, which display only σ-bonding Ru(III)-L are stable.[4,23]

Taking into consideration the fact that CO is a stronger π-acceptor than triethyl phosphite,[14] the photoaquation of CO rather than phosphite along the *z* axis is an apparent contradiction with the observations made on the *cis*-$[Ru(NH_3)_4(isn)L]^{2+}$ [8-10] systems where the weaker π-back-bonding ligand is preferentially labilized. In the $[Rh(NH_3)_5py\text{-}X]^{3+}$ systems[25] in which there is no back-bonding, the exclusive aquation of py-X, which is a weaker σ-donor than NH_3, must come from depopulation of a nonbonding $d\pi$ orbital to a σ^* orbital along the *z* axis. For *cis*-$[Ru(NH_3)_4(isn)L]^{2+}$, the depopulation of a nonbonding $d\pi$ orbital and population of a σ^* orbital would not affect back-bonding;[8-10] thus, the weaker π-back-bonding ligand will be the one more easily labilized.

The photochemical behavior of the *trans*-$[Ru(NH_3)_4P(OEt)_3CO]^{2+}$ complex illustrates well that all molecular orbitals in the valence shell should be taken into account in order to explain photochemical reactivity.

Investigations on related systems are in course and will be reported soon.

Acknowledgment. We are grateful to the Brazilian agencies FAPESP, CAPES, CNPq, and PADCT, for grants and fellowships. We thank Drs. P. C. Ford and J. F. Endicott for helpful discussions and G. Chiericato, Jr., for the use of the CV-1B apparatus.

Registry No. pz, 290-37-9; *trans*-$[Ru(NH_3)_4P(OEt)_3H_2O]^{2+}$, 64939-03-3; *trans*-$[Ru(NH_3)_4(P(OEt)_3)_2]^{2+}$, 64939-00-0; *trans*-$[Ru(NH_3)_4P(OEt)_3CO]^{2+}$, 112786-14-8; $P(OEt)_3$, 122-52-1; CO, 630-08-0; NH_3, 7664-41-7; *trans*-$[Ru(NH_3)_4P(OEt)_3(pz)]^{2+}$, 64939-09-9.

(21) Lim, H. S.; Barclay, D. J.; Anson, F. C. *Inorg. Chem.*, **1972**, *11*, 1460.
(22) Mazzetto, S. E. Master's Thesis, IFQSC-Universidade de São Paulo, São Carlos-SP, Brazil, 1991.
(23) Rezende, N. M. S.; Martins, S. C.; Marinho, L. A.; Santos, J. A. V.; Tabak, M.; Perussi, J. R.; Franco, D. W. *Inorg. Chim. Acta* **1991**, *182*, 87.
(24) Armor, J. N.; Taube, H. *J. Am. Chem. Soc.* **1970**, *92*, 6170.
(25) Peterson, J. D.; Watts, R. J.; Ford, P. C. *J. Am. Chem. Soc.* **1976**, *98*, 3188.

Notes

Contribution from the Department of Chemistry, Pohang Institute of Science and Technology, and Chemistry Group, Research Institute of Industrial Science and Technology, P.O. Box 125, Pohang 790-600, Republic of Korea

Convenient Synthesis, Structure, and Properties of $[(HB(pz)_3)FeCl_3]^-$ [1]

Sung-Hee Cho, Dongmok Whang, Kyu-Nam Han, and Kimoon Kim*

Received May 29, 1991

Introduction

Modeling of active sites of non-heme iron proteins has been one of the active research topics in bioinorganic chemistry in recent years.[2] Tripodal nitrogen ligands $HB(pz)_3^-$ and 1,4,7-triazacyclononane (TACN) (or 1,4,7-trimethyl-1,4,7-triazacyclononane (Me_3TACN)) have been successfully employed in the synthesis of the structural models of methemerythrin, $[Fe_2O(O_2CCH_3)_2L_2]$ (where L = $HB(pz)_3^-$,[3] TACN, or Me_3TACN[4]). While mononuclear complexes $LFeCl_3$ where L = TACN or Me_3TACN were known to be good starting materials for the syntheses of various oxo/hydroxo-bridged multinuclear iron complexes,[4,5] the corre-

* To whom correspondence should be addressed at the Pohang Institute of Science and Technology.

(1) (a) Part of this work has been presented at the 65th Annual Meeting of the Korean Chemical Society, Seoul, Korea. April 13-14, 1990. (b) Abstracted from the M.S. thesis of S.-H.C., Pohang Institute of Science and Technology, December, 1990.
(2) (a) Que, L., Jr.; Scarrow, R. C. In *Metal Clusters in Proteins*; Que, L. Jr., Ed.; ACS Symposium Series 372; American Chemical Society: Washington, DC, 1988; pp 159-178. (b) Lippard, S. J. *Angew. Chem., Int. Ed. Engl.* **1988**, *27*, 344-361.
(3) (a) Armstrong, W. H.; Lippard, S. J. *J. Am. Chem. Soc.* **1983**, *105*, 4837-4838. (b) Armstrong, W. H.; Spool, A.; Papaefthymiou, G. C.; Frankel, R. B.; Lippard, S. J. *Ibid.* **1984**, *106*, 3653-3667.
(4) (a) Wieghardt, K.; Pohl, K.; Gebert, W. *Angew. Chem., Int. Ed. Engl.* **1983**, *22*, 727. (b) Hartman, J. R.; Rardin, R. L.; Chaudhuri, P.; Pohl, K.; Wieghardt, K.; Nuber, B.; Weiss, J.; Papaefthymiou, G. C.; Frankel, R., B.; Lippard, S. J. *J. Am. Chem. Soc.* **1987**, *109*, 7387-7396.
(5) (a) Wieghardt, K.; Pohl, K.; Ventur, D. *Angew. Chem., Int. Ed. Engl.* **1985**, *24*, 392-393. (b) Drueke, S.; Wieghardt, K.; Nuber, B.; Weiss, J.; Fleischhauer, H.-P.; Gehring, S.; Haase, W. *J. Am. Chem. Soc.* **1989**, *111*, 8622-8631. (c) Drueke, S.; Wieghardt, K.; Nuber, B.; Weiss, J. *Inorg. Chem.* **1989**, *28*, 1414-1417. (d) Drueke, S.; Wieghardt, K.; Nuber, B.; Weiss, J.; Bominaar, E. L.; Sawaryn, A.; Winkler, H.; Trautwein, A. X. *Ibid.* **1989**, *28*, 4477-4483.

0020-1669/92/1331-0519$03.00/0

sponding complex with $HB(pz)_3^-$ ligand was not reported until recently. The strong tendency of $HB(pz)_3^-$ to form stable full-sandwich complex FeL_2 is responsible for the difficulty in preparing the half-sandwich complex. In the course of preparing new (μ-oxo)diiron complexes, we have recently isolated the half-sandwich complex $[Et_4N][(HB(pz)_3)FeCl_3]$ (**1**) from the reaction of $[Et_4N][Fe_2OCl_6]$ with $KHB(pz)_3$.[1] In the middle of our investigation of the synthetic utility of **1**, Fukui et al. reported[6] synthesis of **1** by the same reaction. However, they reported that (i) the half-sandwich complex **1** could not be obtained from a more straightforward route, the reaction of $FeCl_3$ with $HB(pz)_3^-$, and (ii) attempts to synthesize the μ-oxo binuclear complex $[Fe_2O(O_2CCH_3)_2(HB(pz)_3)_2]$ by treating **1** with NaOAc failed. In contrast to their report we discovered that the reaction of $FeCl_3$ with $HB(pz)_3^-$ *does* yield the half-sandwich complex **1** and this *is* a useful starting material for the synthesis of the binuclear iron complex. Here we report the details of the discovery and the crystal structures of $[Fe(HB(pz)_3)_2][(HB(pz)_3)FeCl_3]$ (**2**) and $[Fe_2O(O_2CCH_3)_2(HB(pz)_3)_2]\cdot 4CH_3CN$ (**3**) (at −84 °C).

Experimental Section

All reagents were used as received. $KHB(pz)_3$[7] and $[Et_4N][Fe_2OCl_6]$[8] were synthesized by the literature methods. UV–vis and IR spectra were recorded on a Hewlett-Packard 8452A UV–vis spectrometer and a Perkin-Elmer 843 IR spectrometer, respectively. Elemental analyses were performed in the Korea Basic Science Center. Solid-state magnetic susceptibilities were measured with a Johnson Matthey magnetic susceptibility balance. Solution susceptibilities were determined by the NMR method[9] with a Brucker AM 300-MHz spectrometer.

$[Et_4N][(HB(pz)_3)FeCl_3]$ (1). Method A. A solution of 0.500 g (2.00 mmol) of $KHB(pz)_3$ in 20 mL of CH_3CN was added dropwise to a brown suspension containing 0.600 g (1.00 mmol) of $[Et_4N][Fe_2OCl_6]$ in 30 mL of CH_3CN with vigorous stirring. After 4 h of stirring, the volume of the reaction mixture was reduced to ~3 mL by rotary evaporation. After THF (20 mL) was added, the mixture was filtered quickly to remove insoluble solids. The filtrate was kept in a refrigerator for a day to yield yellow solids of **1**, which were recrystallized from CH_2Cl_2 and ether (0.192 g, 19%). UV–vis (MeCN): λ_{max} (ϵ) 367 (10 400), 266 (10 700) nm. IR (KBr, cm^{-1}): 3100 (sh), 3090 (m), 2980 (w), 2480 (m, BH), 1490 (s), 1470 (s), 1390 (s), 1210 (s), 1120 (s), 1040 (s), 970 (m), 780 (s), 720 (s), 660 (m), 630 (m), 280 (m). Anal. Calcd for $C_{17}H_{30}N_7BCl_3Fe$: C, 40.39; H, 5.98; N, 19.40. Found: C, 40.40; H, 6.00; N, 19.20.

Method B. A solution of 0.50 g (2.0 mmol) of $KHB(pz)_3$ in 25 mL of methanol was added dropwise to a yellow solution of $FeCl_3\cdot 6H_2O$ (0.54 g, 2.0 mmol) in 25 mL of methanol with vigorous stirring. After the solution was stirred for 4 h, Et_4NCl (0.33 g; 2.0 mmol) was added to the solution. The resulting solution was stirred for additional 1 h and evaporated to dryness. The residue was taken up to 20 mL of acetonitrile and filtered to remove insoluble solids. The volume of the filtrate was reduced to ~5 mL and THF (20 mL) was added to the solution. Leaving the solution overnight at room temperature yielded microcrystals of **1**. The first crop was collected by filtration, and the filtrate was concentrated and allowed to stand in a refrigerator to produce a second crop. The combined crops were recrystallized from CH_2Cl_2 and ether (0.212 g, 21%). Anal. Calcd for $C_{17}H_{30}N_7BCl_3Fe$: C, 40.39; H, 5.98; N, 19.40. Found: C, 40.66; H, 5.68; N, 19.23.

$[Fe(HB(pz)_3)_2][(HB(pz)_3)FeCl_3]$ (2). Dark red crystals of **2** (along with crystals of $[Fe(HB(pz)_3)_2]Cl$) were obtained adventitiously from the reaction mixture of $KHB(pz)_3$ and $[Et_4N][Fe_2OCl_6]$ in CH_3CN. Compound **2** was characterized by X-ray crystallography (see below). Attempts to prepare pure **2** by mixing equimolar quantities of $[Fe(HB(pz)_3)_2](NO_3)$[10] and $[Et_4N][(HB(pz)_3)FeCl_3]$ followed by selective crystallizations under various conditions have not been successful.

$[Fe_2O(O_2CCH_3)_2(HB(pz)_3)_2]\cdot 4CH_3CN$ (3). Sodium acetate trihydrate (113 mg, 0.83 mmol) was added to a solution of **1** (84 mg, 0.166 mmol) in 10 mL of acetonitrile. The resulting suspension was stirred for 3 days. During this period the red suspension turned to greenish brown. Brown precipitates were filtered off, and the filtrate was concentrated and allowed to stand in the freezer (−10 °C) for 4 days to produce greenish brown crystals of **3** (yield: 34 mg, 30%). UV–vis spectrum of the product was identical with the one reported by Armstrong et al.[3] UV–vis (CH_3CN): λ_{max} 270, 338, 365 (sh), 462, 488, 520 (sh) nm. Anal. Calcd for $C_{22}H_{26}N_{12}O_5B_2Fe_2$: C, 39.29; H, 3.87, N, 25.00. Found: C, 39.05; H, 3.60; N, 24.82. The identity of the product was also confirmed by single-crystal X-ray diffraction methods.

Table I. Crystallographic Data for **2** and **3**

	2	**3**
formula	$C_{27}H_{30}N_{18}B_3Cl_3Fe_2$	$C_{30}H_{38}N_{16}O_5B_2Fe_2$
fw	857.15	836.06
space group	$P2_1/n$ (No. 14)	*Pnma* (No. 62)
a, Å	12.063 (1)	15.752 (1)
b, Å	21.859 (2)	19.785 (2)
c, Å	14.121 (2)	12.872 (1)
β, deg	97.77 (1)	
vol, Å^3	3689.1 (7)	4011.7 (6)
Z	4	4
temp, °C	23	−84
d(calc), g cm^{-3}	1.543	1.384
radiation	graphite-monochromated Mo Kα(λ(Kα_1) = 0.709 26 Å)	
linear abs coeff, cm^{-1}	10.5	7.8
2θ limits, deg	$6 < 2\theta < 50$	$6 < 2\theta < 40.4$
no. of unique data with $I > 3\sigma(I)$	4422	1250
R^a	0.038	0.069
R_w^b	0.041	0.075

$^a R = \sum||F_o| - |F_c||/\sum|F_o|$. $^b R_w = [\sum w(|F_o| - |F_c|)^2/\sum w|F_o|^2]^{1/2}$; $w = 4F_o^2/\sigma^2(F_o^2)$; $\sigma(F_o^2) = [\sigma(I) + (pI)^2]^{1/2}$.

X-ray Crystal Structure Determination of 2 and 3. X-ray data were collected on an Enraf-Nonius CAD4 diffractometer using Mo Kα radiation at room temperature for **2** and at −84 °C for **3** as crystals of **3** decomposed rapidly at room temperature when they were taken out of the mother liquor. Cell parameters and an orientation matrix for data collection were obtained from least-squares refinement, using the setting angles of 25 reflections in the range $20.0 < 2\theta < 30.0$. The crystallographic data are summarized in Table I. The intensities of three standard reflections, recorded every 3 h of X-ray exposure, showed no systematic changes. All the calculations were carried out with the Enraf-Nonius Structure Determination Package (SDP). The intensity data were corrected for Lorentz and polarization effects, and empirical absorption corrections were also applied. The structures were solved by a combination of Patterson and difference Fourier methods and refined by full-matrix least-squares methods. All the non-hydrogen atoms were refined anisotropically for **2**. Owing to the small number of data with $I > 3\sigma(I)$, only Fe, O, and N atoms were refined anisotropically for **3**. The positions of hydrogen atoms were idealized (d(C–H) = 0.95 Å) and included in the calculations of the structure factors as fixed contributions. Each hydrogen atom was assigned an isotropic thermal parameter of 1.2 times that of attached atom. The final cycle of refinement led to the R indices listed in Table I. The atomic scattering factors were taken from ref 11 for the non-hydrogen atoms and from the literature[12] for hydrogen. The final positional and anisotropic thermal parameters and complete bond distances and angles for **2** and **3** are available as supplementary material.

Results and Discussion

Preparation of $[Et_4N][(HB(pz)_3)FeCl_3]$. At the outset of this work we hoped to obtain the μ-oxo diiron complex $LFeO(HCO_3)_2FeL$ ($L = HB(pz)_3$) from the reaction of $[Et_4N][Fe_2OCl_6]$ with $HB(pz)_3^-$ in CH_3CN containing $NaHCO_3$. Instead, the reaction produced $[Fe(HB(pz)_3)_2]^+$ as a major product, and $[(HB(pz)_3)FeCl_3]^-$ as a minor product. Since the half-sandwich anion complex is much less soluble in THF than the full-sandwich cation complex, one can isolate **1** selectively from the THF solution of the reaction mixture. Recrystallization of the crude product from CH_2Cl_2/ether yields analytically pure **1**.[13]

In contrast to Fukui et al.'s report,[6] however, we found that the half-sandwich complex can be synthesized by a more

(6) Fukui, H.; Ito, M.; Moro-oka, Y.; Kitajima, N. *Inorg. Chem.* **1990**, *29*, 2868–2870.
(7) Trofimenko, S. *Inorg. Synth.*, **1970**, *12*, 99–109.
(8) Armstrong, W. H.; Lippard, S. J. *Inorg. Chem.* **1985**, *24*, 981–982.
(9) Evans, D. F. *J. Chem. Soc.* **1958**, 2003–2005.
(10) Cho, S.-H.; Whang, D.; Kim, K. *Bull. Kor. Chem. Soc.* **1991**, *12*, 107–109.
(11) *International Tables for X-ray Crystallography*; Kynoch: Birmingham, England, 1974; Vol. IV, pp 99 and 149.
(12) Stewart, R. F.; Davison, E. R.; Simpson, W. T. *J. Chem. Phys.* **1965**, *42*, 3175–3187.
(13) We also determined the X-ray crystal structure[1] of **1**, which is identical with the one reported by Fukui et al.[6] within experimental error. However, we noticed that the reported[6] λ_{max} values of the UV–visible spectrum of **1** (in CH_3CN) are somewhat different from ours.

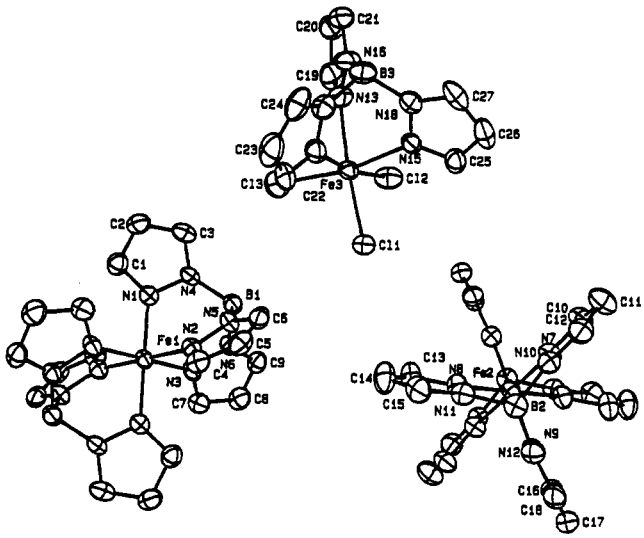

Figure 1. Structure of 2 showing two crystallographically independent $[Fe(HB(pz)_3)_2]^+$ cations, each of which has an inversion symmetry, and a $[(HB(pz)_3)FeCl_3]^-$ anion.

Table II. Selected Bond Distances (Å) and Angles (deg) for $[Fe(HB(pz)_3)_2][(HB(pz)_3)FeCl_3]$ (2)

Fe1-N1	1.961 (3)	Fe3-Cl1	2.319 (1)
Fe1-N2	1.959 (3)	Fe3-Cl2	2.316 (1)
Fe1-N3	1.945 (3)	Fe3-Cl3	2.305 (1)
Fe2-N7	1.945 (3)	Fe3-N13	2.159 (4)
Fe2-N8	1.975 (3)	Fe3-N14	2.161 (4)
Fe2-N9	1.952 (4)	Fe3-N15	2.197 (3)
N1-Fe1-N2	88.9 (1)	Cl1-Fe3-N15	90.2 (1)
N1-Fe1-N3	88.7 (1)	Cl2-Fe3-N13	89.7 (1)
N2-Fe1-N3	88.5 (1)	Cl2-Fe3-N14	169.8 (1)
N7-Fe2-N8	88.1 (1)	Cl2-Fe3-N15	90.7 (1)
N7-Fe2-N9	88.1 (1)	Cl3-Fe3-N13	90.7 (1)
N8-Fe2-N9	88.7 (1)	Cl3-Fe3-N14	90.9 (1)
Cl1-Fe3-Cl2	96.23 (5)	Cl3-Fe3-N15	168.47 (9)
Cl1-Fe3-Cl3	97.45 (5)	N13-Fe3-N14	83.8 (1)
Cl2-Fe3-Cl3	96.97 (6)	N13-Fe3-N15	80.7 (1)
Cl1-Fe3-N13	169.2 (1)	N14-Fe3-N15	80.5 (1)
Cl1-Fe3-N14	89.1 (1)		

straightforward route, the reaction of $FeCl_3 \cdot 6H_2O$ and $KHB(pz)_3$ in methanol followed by a similar workup. Since the formation of $[Fe(HB(pz)_3)_2]^+$ was also dominant in this procedure, the yield was no better than that of the method using $[Fe_2OCl_6]^-$ as starting material. However, this route offers great advantage over the previous one as it requires only inexpensive, commercial reagents and allows large-scale preparation of the potentially useful starting material. $[(HB(pz)_3)FeCl_3]^-$ in CH_3CN solution slowly decomposes into $[Fe(HB(pz)_3)_2]^+$ and $FeCl_4^-$ as determined by UV-visible spectroscopy. Magnetic susceptibilities of **1** measured at room temperature in solution (μ_{eff} = 6.04 μ_B) and in the solid state (μ_{eff} = 5.68 μ_B) are consistent with high-spin Fe(III).

X-ray Crystal Structure of $[Fe(HB(pz)_3)_2][(HB(pz)_3)FeCl_3]$. At an early stage of this work we obtain adventitiously dark red crystals from the reaction mixture of $[Et_4N][Fe_2OCl_6]$ with $HB(pz)_3^-$ in CH_3CN. X-ray crystal structure analysis revealed that the compound is $[Fe(HB(pz)_3)_2][(HB(pz)_3)FeCl_3]$, the structure of which is shown in Figure 1. The asymmetric unit of the crystal contains two crystallographically independent $[Fe(HB(pz)_3)_2]^+$ cations, each of which occupies an inversion center, and a $[(HB(pz)_3)FeCl_3]^-$ anion, which takes a general position. Selected bond distances and angles are given in Table II. The structures of the two cations are nearly identical. The coordination geometry around the Fe(III) ion of the cation is close to a regular octahedron. The average Fe-N distance (1.956 (10)[14] Å) and average N-Fe-N angle (88.5 (3)°) are in good agreement with those for the low-spin $Fe(HB(pz)_3)_2^+$ structures reported in the literature.[3b,10] The structure of the anion is similar to that of the anion of high-spin $[Et_4N][Fe(HB(pz)_3)Cl_3]$.[1,6] The average Fe-N and Fe-Cl distances are 2.172 (17)[14] and 2.313 (6)[14] Å, respectively. One of the Fe-N bond distances (Fe3-N15) is significantly longer (0.037 Å) than the other two. Also, the Fe-Cl bond trans to this longer Fe-N bond is shorter (~0.012 Å) than the other two Fe-Cl bonds. A similar structural behavior is also observed in the anion of **1**.[1,6] The origin of such large variation in distances of apparently equivalent bonds is not clear. Structural parameters of the $HB(pz)_3$ ligands in both cation and anion are not exceptional. This compound is probably the first structurally characterized iron complex containing both high-spin and low-spin six-coordinate Fe(III) ions.

(14) The number in parentheses following an average value is the estimated standard deviation calculated on the assumption that the individual measurements are drawn from the same population.

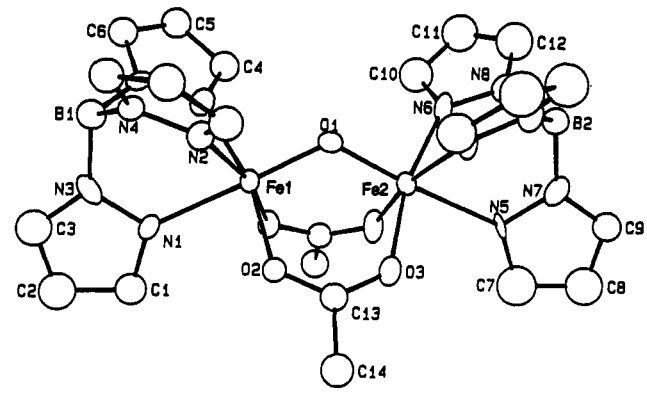

Figure 2. Structure of 3 with the atom-labeling scheme.

Table III. Selected Bond Distances (Å) and Angles (deg) for $[Fe_2O(O_2CCH_3)_2(HB(pz)_3)_2] \cdot 4CH_3CN$ (3)

Fe1···Fe2	3.144 (2)		
Fe1-O1	1.787 (10)	Fe2-O1	1.787 (10)
Fe1-O2	2.038 (8)	Fe2-O3	2.037 (9)
Fe1-N1	2.194 (14)	Fe2-N5	2.190 (13)
Fe1-N2	2.148 (9)	Fe2-N6	2.144 (10)
Fe1-O1-Fe2	123.3 (6)		
O1-Fe1-O2	97.1 (3)	O1-Fe2-O3	97.0 (3)
O1-Fe1-N1	177.9 (5)	O1-Fe2-N5	175.8 (5)
O1-Fe1-N2	95.9 (3)	O1-Fe2-N6	95.4 (3)
O2-Fe1-N1	84.4 (3)	O3-Fe2-N5	86.0 (3)
O2-Fe1-N2	166.5 (3)	O3-Fe2-N6	167.5 (4)
N1-Fe1-N2	82.5 (4)	N5-Fe2-N6	81.5 (4)

Preparation of $[Fe_2O(O_2CCH_3)_2(HB(pz)_3)_2]$ Using $[Et_4N][Fe(HB(pz)_3)Cl_3]$. In contrast to Fukui et al.'s report,[6] we were able to prepare the μ-oxo binuclear complex **3** in a moderate yield by treating **1** with $NaOAc \cdot 3H_2O$ in CH_3CN although the conversion was slow in part due to poor solubility of NaOAc in CH_3CN. The product was identified by comparing its UV-vis spectrum with that of the authentic sample[3a] and also by X-ray crystallography. The present crystal structure, which was determined at -84 °C, was different from that at room temperature:[3a] The present structure has a higher space group symmetry (orthorhombic *Pnma* vs monoclinic $P2_1/n$ for the room-temperature structure), which imposes mirror planes on one of which the $[Fe_2O(O_2CCH_3)_2(HB(pz)_3)_2]$ complex lies. The mirror plane contains two Fe atoms, the oxo, 2 B atoms, and 2 pz rings (Figure 2). Structural parameters of the $[Fe_2O(O_2CCH_3)_2(HB(pz)_3)_2]$ complex are in good accord with those of the room-temperature structure[3] within the rather large experimental error of the present structure. Selected bond distances and angles are listed in Table III.

In summary, we discovered a straightforward method to prepare the half-sandwich complex $[Fe(HB(pz)_3)Cl_3]^-$, by the reaction of $FeCl_3$ with $HB(pz)_3^-$, and successful preparation of **2** using this complex illustrates that **1** can be a useful starting material for the synthesis of multinuclear iron complexes. Further investigation of the synthetic utility of **1** is currently in progress.

Acknowledgment. We gratefully acknowledge financial support from the Research Institute of Industrial Science and Technology

(RIST). We also thank Mr. Sang-Yong Lee for his help at the early stage of this work.

Registry No. 1, 128302-30-7; 2, 137822-83-4; 3, 86177-71-1; $[Et_4N][Fe_2OCl_6]$, 87495-23-6.

Supplementary Material Available: Tables of positional and isotropic thermal parameters, anisotropic thermal parameters, and complete bond distances and angles for 2 and 3 (16 pages); tables of structure factors for 2 and 3 (30 pages). Ordering information is given on any current masthead page.

Contribution from the Department of Chemistry, University of Texas at El Paso, El Paso, Texas 79968-0513, and Central Research Institute of Chemistry, Hungarian Academy of Sciences, H-1525 Budapest, P.O. Box 17, Hungary

The Germanium-Tin Bond. Structures of the Isomeric Complexes Me_3E-$E'Ph_3$ (E = Ge, E' = Sn; E = Sn, E' = Ge)

Keith H. Pannell,*,† László Párkányi,‡ Hemant Sharma,† and Francisco Cervantes-Lee†

Received July 26, 1991

Introduction

A compound containing a Ge-Sn bond was initially reported in 1927 by Kraus and Foster, $Ph_3GeSnMe_3$ (II); much later Gilman and Gerow reported $Ph_3GeSnPh_3$, and Creemers and Noltes reported several oligomeric germylstannanes.[1,2] However, there has been limited study on such compounds. Chambers and Glockling determined heats of formation and bond dissociation energies from appearance potential measurements[3] and also studied the mass spectral fragmentation patterns of such compounds in which significant ligand exchange between the two metals was observed.[4] Carey and Clark studied the far-infrared spectra of these compounds and assigned metal-metal stretching frequencies for the Ge-Sn bond in the range 225-235 cm^{-1}.[5] Chemical studies on such bonds by Kraus and Foster showed that II underwent homolytic cleavage of the Ge-Sn bond when reacted with bromine. Optically active Ge-Sn compounds with activity at both Ge and Sn have also been reported.[6]

Whereas much crystallographic data have been published concerning the nature of the homonuclear group 14 bonds, Si-Si,[7,8] Ge-Ge,[9] Sn-Sn,[10] and Pb-Pb,[11] reports concerning heteronuclear intra group 14 bonding are rare, totaling only nine examples, Si-Ge,[12] Si-Sn,[13] Ge-Pb,[14] and Sn-Pb.[14] There are no examples of a Ge-Sn-bonded compound, although Adams and Dräger have published the space group and cell constants of $Ph_3SnGePh_2SnPh_3$ but were unable to obtain crystals suitable for total structural analysis.[13b] A series of Ph_3PbEPh_3 complexes (E = Ge, Sn, Pb) have been structurally characterized, but it was not possible to positively distinguish the two different group 14 metal atoms.[14] We recently reported that the isomeric pair of compounds $Me_3SiGePh_3$ and $Ph_3SiGeMe_3$ possess significantly different bond lengths and suggested that a simple explanation for this difference involved expansion and contraction of valence orbitals by electron-donating or -withdrawing substituents that permitted more energetically favorable overlap.[12b] If correct, this explanation should apply to a general class of inorganic systems containing ligand-exchanged isomers.

We have now structurally characterized the Ge-Sn bonds in the isomeric compounds $Me_3GeSnPh_3$ (I) and $Ph_3GeSnMe_3$ (II) and wish to report the results of this study to provide first-time values for the Ge-Sn bond length and furthermore to show that the simple ideas promulgated to explain the bond length differences in the isomeric Ge-Si compounds hold for the intermetallic bonds in isomers I and II.

Table I. Structure Determination Summary

	I	II
empirical formula	$C_{21}H_{24}GeSn$	$C_{21}H_{24}GeSn$
color; habit	colorless; fragment	colorless; prism
cryst size, mm	0.24 × 0.40 × 0.22	0.42 × 0.36 × 0.60
cryst system	orthorhombic	orthorhombic
space group	$Pna2_1$	$Pna2_1$
unit cell dimens		
a, Å	20.634 (2)	20.395 (4)
b, Å	12.394 (2)	12.412 (2)
c, Å	8.0340 (10)	8.085 (2)
V, Å^3	2054.6 (5)	2046.7 (7)
Z	4	4
fw	467.7	467.7
density (calc), Mg/m^3	1.512	1.518
abs coeff, mm^{-1}	2.662	2.672
F(000)	928	928
no. of reflns collected	1076	1069
no. of indep reflns	1034 (R_{int} = 0.00%)	1027 (R_{int} = 0.00%)
no. of obs reflns	814 ($F > 3.0\sigma(F)$)	869 ($F > 3.0\sigma(F)$)
final R, R_w (obs data)	3.02%, 3.95%	2.63%, 3.31%
R, R_w (all data)	4.40%, 4.92%	3.45%, 3.54%

Table II. Selected Bond Lengths (Å) and Angles (deg)

	I	II
Ge-Sn	2.599 (3)	2.652 (2)
Ge-C	1.969 (19) (C19)	1.929 (13) (C1)
	1.973 (19) (C21)	1.940 (12) (C7)
	1.947 (17) (C20)	1.924 (13) (C13)
Sn-C	2.143 (17) (C1)	2.191 (16) (C19)
	2.161 (14) (C7)	2.173 (14) (C21)
	2.162 (17) (C13)	2.137 (17) (C20)

I		II	
Cl-Sn-C7	107.2 (6)	C20-Sn-C21	107.5 (6)
C19-Ge-C20	109.0 (9)	Cl-Ge-C13	109.4 (6)
Sn-Ge-C19	110.7 (9)	Sn-Ge-Cl	109.6 (6)
Ge-Sn-Cl	111.1 (7)	Ge-Sn-C20	110.3 (6)

(1) Kraus, C. A.; Foster, L. S. *J. Am. Chem. Soc.* **1927**, *9*, 457.
(2) (a) Gilman, H.; Gerow, W. *J. Org. Chem.* **1957**, *22*, 334. (b) Creemers, H. M. J. C.; Noltes, J. G. *J. Organomet. Chem.* **1967**, *7*, 237.
(3) Chambers, D. B.; Glockling, F. *Inorg. Chim. Acta* **1970**, *4*, 150.
(4) Chambers, D. B.; Glockling, F. *J. Chem. Soc. A* **1968**, 735.
(5) Carey, N. A. D.; Clark, H. C. *J. Chem. Soc., Chem. Commun.* **1967**, 292.
(6) Gielen, M.; Simon, S.; Tondeur, Y.; Van de Steen, M.; Hoogzand, C.; Van den Eynde, I. *Isr. J. Chem.* **1976/7**, *15*, 74.
(7) Examination of the Cambridge Crystal Structure data base, up to 1987, revealed the following number of structures containing E-E' bonds: E-E' = Si_2, >100; E-E' = Ge_2, 32; E-E' = Sn_2, 45; E-E' = Pb_2, 7; E-E' = SiGe, 3; E-E' = SiSn, 2; E-E' = SiPb, 0; E-E' = GeSn, 0; E-E' = GePb, 1; E-E' = SnPb, 2.
(8) (a) Wojnowski, W.; Peters, K.; Peters, E.-M.; von Schnering, H. G.; Becker, B. *Z. Anorg. Allg. Chem.* **1987**, *553*, 287. (b) Wojnowski, W.; Dreczewski, B.; Peters, K.; Peters, E.-M.; von Schnering, H. G. *Z. Anorg. Allg. Chem.* **1986**, *540/541*, 271. (c) Wiberg, N.; Schuster, H.; Simon, A.; Peters, K. *Angew. Chem., Int. Ed. Engl.* **1986**, *25*, 79. (d) Parkanyi, L.; Hengge, E. *J. Organomet. Chem.* **1982**, *235*, 273. (e) Drahnak, J.; West, R.; Calabrase, J. C. *J. Organomet. Chem.* **1980**, *198*, 55. (f) Parkanyi, L.; Pannell, K. H.; Hernandez, C. *J. Organomet. Chem.* **1983**, *252*, 127.
(9) (a) Haberle, K.; Dräger, M. *Z. Naturforsch., B* **1987**, *42*, 323. (b) Haberle, K.; Dräger, M. *J. Organomet. Chem.* **1986**, *312*, 155. (c) Ross, L.; Dräger, M. *Z. Anorg. Allg. Chem.* **1981**, *472*, 109. (d) Ross, L.; Dräger, M. *Z. Anorg. Allg. Chem.* **1984**, *519*, 225. (e) Bochova, R. I.; Drozdov, Yu. N.; Kuzman, E. A.; Buchkarev, M. N. *Koord. Chim.* **1987**, *13*, 1126.
(10) (a) Adams, S.; Dräger, M.; Mathiasch, B. *Z. Anorg. Allg. Chem.* **1986**, *532*, 81. (b) Adams, S.; Dräger, M.; Mathiasch, B. *J. Organomet. Chem.* **1987**, *326*, 173. (c) Faggiani, R.; Johnson, J. P.; Brown, I. D.; Burchall, T. *Acta Crystallogr., Sect. B* **1979**, *35*, 1227.
(11) (a) Huber, F.; Preut, H. *Z. Anorg. Allg. Chem.* **1976**, *419*, 92. (b) Kleiner, N.; Dräger, M. *Z. Naturforsch., B* **1985**, *40*, 477. (c) Critchlow, S. C.; Corbett, J. D. *Inorg. Chem.* **1985**, *24*, 979.
(12) (a) Párkányi, L.; Hernandez, C.; Pannell, K. H. *J. Organomet. Chem.* **1986**, *301*, 145. (b) Pannell, K. H.; Kapoor, R. N.; Raptis, R.; Párkányi, L.; Fülöp, V. *J. Organomet. Chem.* **1990**, *384*, 41. (c) Mallela, S. P.; Geanangel, R. A. *Inorg. Chem.* **1991**, *30*, 1480.

† University of Texas at El Paso.
‡ Hungarian Academy of Sciences.

0020-1669/92/1331-0522$03.00/0